Archives of Biochemistry and Biophysics
Vol. 382, No. 1, October 1, pp. 105–112, 2000
doi:10.1006/abbi.2000.2021, available online at http://www.idealibrary.com on IDEAL®

Site-Directed Mutagenesis Improves Catalytic Efficiency and Thermostability of *Escherichia coli* pH 2.5 Acid Phosphatase/Phytase Expressed in *Pichia pastoris*

Eric Rodriguez,* Zachary A. Wood,† P. Andrew Karplus,† and Xin Gen Lei*,[1]
Department of Animal Science, Cornell University, Ithaca, New York 14853; and †Department of Biochemistry and Biophysics, Oregon State University, Corvallis, Oregon 97331

Received May 15, 2000, and in revised form July 7, 2000

***Escherichia coli* pH 2.5 acid phosphatase gene (*appA*) and three mutants were expressed in *Pichia pastoris* to assess the effect of strategic mutations or deletion on the enzyme (EcAP) biochemical properties. Mutants A131N/V134N/D207N/S211N, C200N/D207N/S211N, and A131N/V134N/C200N/D207N/S211N had four, two, and four additional potential N-glycosylation sites, respectively. Extracellular phytase and acid phosphatase activities were produced by these mutants and the intact enzyme r-AppA. The N-glycosylation level was higher in mutants A131N/V134N/D207N/S211N (48%) and A131N/V134N/C200N/D207N/S211N (89%) than that in r-AppA (14%). Despite no enhancement of glycosylation, mutant C200N/D207N/S211N was different from r-AppA in the following properties. First, it was more active at pH 3.5–5.5. Second, it retained more ($P < 0.01$) phytase activity than that of r-AppA. Third, its specific activity of phytase was 54% higher. Lastly, its apparent catalytic efficiency k_{cat}/K_m for either *p*-nitrophenyl phosphate (5.8×10^5 vs 2.0×10^5 min^{-1} M^{-1}) or sodium phytate (6.9×10^6 vs 1.1×10^6 min^{-1} M^{-1}) was improved by factors of 1.9- and 5.3-fold, respectively. Based on the recently published *E. coli* phytase crystal structure, substitution of C200N in mutant C200N/D207N/S211N seems to eliminate the disulfide bond between the G helix and the GH loop in the α-domain of the protein. This change may modulate the domain flexibility and thereby the catalytic efficiency and thermostability of the enzyme.**

***Key Words: Escherichia coli* acid phosphatase; phytase; mutagenesis; heterologous expression; *Pichia pastoris;* glycosylation; thermostability; catalytic function; protein structure.**

Phytate (*myo-inositol* 1,2,3,4,5,6-hexakisphosphate) is the major form of phosphorus in cereals and legumes (1). Because simple-stomached animals and humans are unable to digest phytate efficiently, supplemental dietary phytase is needed for them to utilize phosphorus and other minerals bound in this compound. *Escherichia coli* pH 2.5 acid phosphatase (EcAP,[2] EC 3.1.3.2), encoded by *appA*, is a periplasmic, monomeric protein of 45 kDa (2). Because of the conserved RHGXRXP active-site motif in the polypeptide, this enzyme belongs to the high molecular weight histidine acid phosphatase family (3–5). Mutagenesis of EcAP has previously demonstrated that a single substitution of His17 by Asn causes a complete loss of its acid phosphatase activity (5). Similarly, the presence of His303 and Asp304 (N-terminal HD motif) is also important for the EcAP activity (4). Recently, we expressed the *appA* gene in yeast *Pichia pastoris* as an active, extracellular enzyme (r-AppA) that degrades sodium phytate (6), in addition to many substrates of acid phosphatases, such as *p*-nitrophenyl phosphate (pNPP), ATP, and fructose 1,6-bisphosphate (4, 5). Importantly, this recombinant enzyme can be used as a supplemental phytase in animal diets to improve phosphorus utilization and to reduce phosphorus pollution from animal waste (7).

The inability of currently available phytase to tolerate heat denaturation from feed processing remains one of the major practical concerns (8). Previous work in our laboratory has demonstrated a positive effect of

[1] To whom correspondence should be addressed. Fax: (607) 255-9829. E-mail: XL20@cornell.edu.

[2] Abbreviations used: BMGY, buffered glycerol–complex medium; BMMY, buffered methanol–complex medium; DEAE, diethylaminoethyl; dNTPs, deoxynucleotides; EcAP, *Escherichia coli* pH 2.5 acid phosphatase; Endo H_f, endoglycosidase H_f; pNPP, *p*-nitrophenyl phosphate; r-AppA, *E. coli* acid phosphatase expressed in *Pichia pastoris;* YPD, yeast extract peptone dextrose.

0003-9861/00 $35.00

TABLE I

Modified Primers and Index of Surface Solvent Accessibility for Mutations

Primer[a]	Position[b]	Primer sequence[c]	Modification[d]	Accessibility[e] (%)
E2 (f)	241–264	5′-GGAATTCGCTCAGAGTGAGCCGGA-3′	*Eco*RI restriction site	—
A1 (r)	565–592	5′-CTGGGTATGGTTGGTTATATTACAGTCAGGT-3′	A131N	1.05
			V134N	0.55
P2 (f)	772–795	5′-CAAACTTGAACCTTAAACGTGAG-3′	C200N	nd
P3 (r)	796–825	5′-CCTGCGTTAAGTTACAGCTTTCATTCTGTTT-3′	D207N	0.63
			S211N	0.65
K2 (r)	1469–1491	5′-GGGGTACCTTACAAACTGCACG-3′	*Kpn*I restriction site	—

[a] f, forward; r, reverse.
[b] Nucleotide position based on the *E. coli* periplasmic pH 2.5 acid phosphatase (GenBank Accession No. M58708).
[c] Underlined nucleotides were substituted.
[d] Amino acid mutation or restriction site added. The coding region starts at the codon 20 and ends at the codon 432. Amino acids A131, V134, C200, D207, and S211 are labeled A109, V112, C178, D185, and S189 by Lim *et al.* (22).
[e] Percentage of amino acid surface solvent accessibility (19, 20); nd, not determined.

N-linked glycosylation on the thermostability of *Aspergillus niger* phytase (*phyA*) expressed in *P. pastoris* and *Saccharomyces cerevisiae* (9, 10). Effects of glycosylation on thermostability and biochemical properties have also been shown in other proteins (11–15). In general, glycosylation is a complex covalent modification of structure and function for secretory proteins in eukaryotes. The carbohydrate groups may have multiple roles in controlling conformation, folding, stability, resistance to proteolysis, modulation of enzyme activity, cell recognition, and appropriate targeting (16, 17). It is possible that additional glycosylation of EcAP may affect its enzymatic properties. Because there are only three putative *N*-glycosylation sites in the *appA* gene (3), it is of interest to determine whether additional glycosylation sites could be engineered to modulate the enzyme thermostability. Therefore, mutagenesis of the *appA* gene was undertaken in the present study. Wild-type *appA* and several mutants were expressed in *P. pastoris* to determine the impact of adding multiple N-glycosylation sites on the thermostability and biochemical properties of r-AppA.

EXPERIMENTAL PROCEDURES

Sequence analysis for designing mutations. Our criteria for designing mutations to enhance glycosylation of EcAP were as follows: (1) the potential glycosylation site should have 25% or greater solvent accessibility, and (2) the site should be easily engineered by a single residue change to give an N-linked glycosylation motif (Asn-X-Ser or Asn-X-Thr, where X is not a proline). Initially, in the absence of a crystal structure for EcAP, we used the crystal structure of rat acid phosphatase (35% sequence identity) (18) to calculate accessibilities as follows. First, we aligned EcAP and rat acid phosphatase to several closely related phosphatases/phytases using the multisequence alignment program PIMA (19). The aligned sequences included human prostatic acid phosphatase precursor (GenBank Accession No. P15309), *Caenorhabditis elegans* histidine acid phosphatase (GenBank Accession No. Z68011), *Aspergillus fumigatus* phytase (GenBank Accession No. U59804), *Pichia angusta* repressible acid phosphatase (GenBank Accession No. AF0511611), rat acid phosphatase (GenBank Accession No. 576257), and *E. coli appA* (GenBank Accession No. M58708). Next, we determined the solvent-accessible surface of all of the amino acids of rat acid phosphatase using the program DSSP (20), converting these values to percent accessibility by dividing the total surface area of the corresponding amino acid as previously described (21). We only considered residues greater than 25% solvent accessible and assigned these values to the corresponding amino acids in EcAP based on the sequence alignment described above, under the assumption that the overall structure of rat acid phosphatase and EcAP would be conserved. Finally, we examined the putative solvent-accessible residues to determine which could be easily converted to an *N*-glycosylation site by point mutation. Out of 31 potential sites, 5 were selected that best fit our criteria. An additional mutation C200N was incorporated using primer P2, designed for another *appA* mutagenesis study. From the alignment performed, the mutation C200N is in a gapped region and C200 is involved with C210 (labeled as C178/C188 by Lim *et al.*, 22) in forming a unique disulfide bond between helix G and the GH loop (an unorganized configuration between the G and H helices) in the α-domain of the protein (22). Correspondingly, five PCR primers were designed: E2 and K2 for amplifying the wild-type sequence of *appA* (3) and the others for developing three mutants (Table I and Fig. 1). All primers were synthesized by the Cornell University Oligonucleotide Synthesis Facility (Ithaca, NY).

Construction of mutants by PCR. The *E. coli appA* mutants were constructed using the megaprimer site-directed mutagenesis method adapted from previous studies (23, 24). To amplify the intact coding region of *appA*, the PCR was set up in a 50-μL final volume containing 200 ng of DNA of *appA* inserted in a pAPPA1 plasmid isolated from *E. coli* strain BL21 (3), 50 pmol of each primer E2 and K2, 5 U of AmpliTaq DNA polymerase (Perkin Elmer, Norwalk, CT), 10 mM Tris–HCl, pH 8.3, 50 mM KCl, 12.5 mM $MgCl_2$, and 200 mM each dNTPs (Promega Corp., Madison, WI). The reaction was performed using the GeneAmp PCR system 2400 (Perkin Elmer) and included 1 cycle at 94°C (3 min), 30 cycles of [94°C (0.5 min), 54°C (1 min), and 72°C (1.5 min)], and 1 cycle at 72°C (10 min). Megaprimers for mutants were produced in a separate round of PCR (Table II). The first mutagenic PCR reaction (100 μL) was performed as described above, using 4 μL of the intact *appA* PCR mixture and the respective modified primers listed in Table I. All megaprimer PCR products were resolved in a 1.5% low-melting agarose (GIBCO BRL, Grand Island, NY) gel electrophoresis. The expected fragments were excised and eluted with the GeneClean II kit (Bio101, Vista, CA). The final mutagenic PCR reaction (100 μL) was set up as described above, using 4 μL of the *appA* PCR product and varying concentrations of

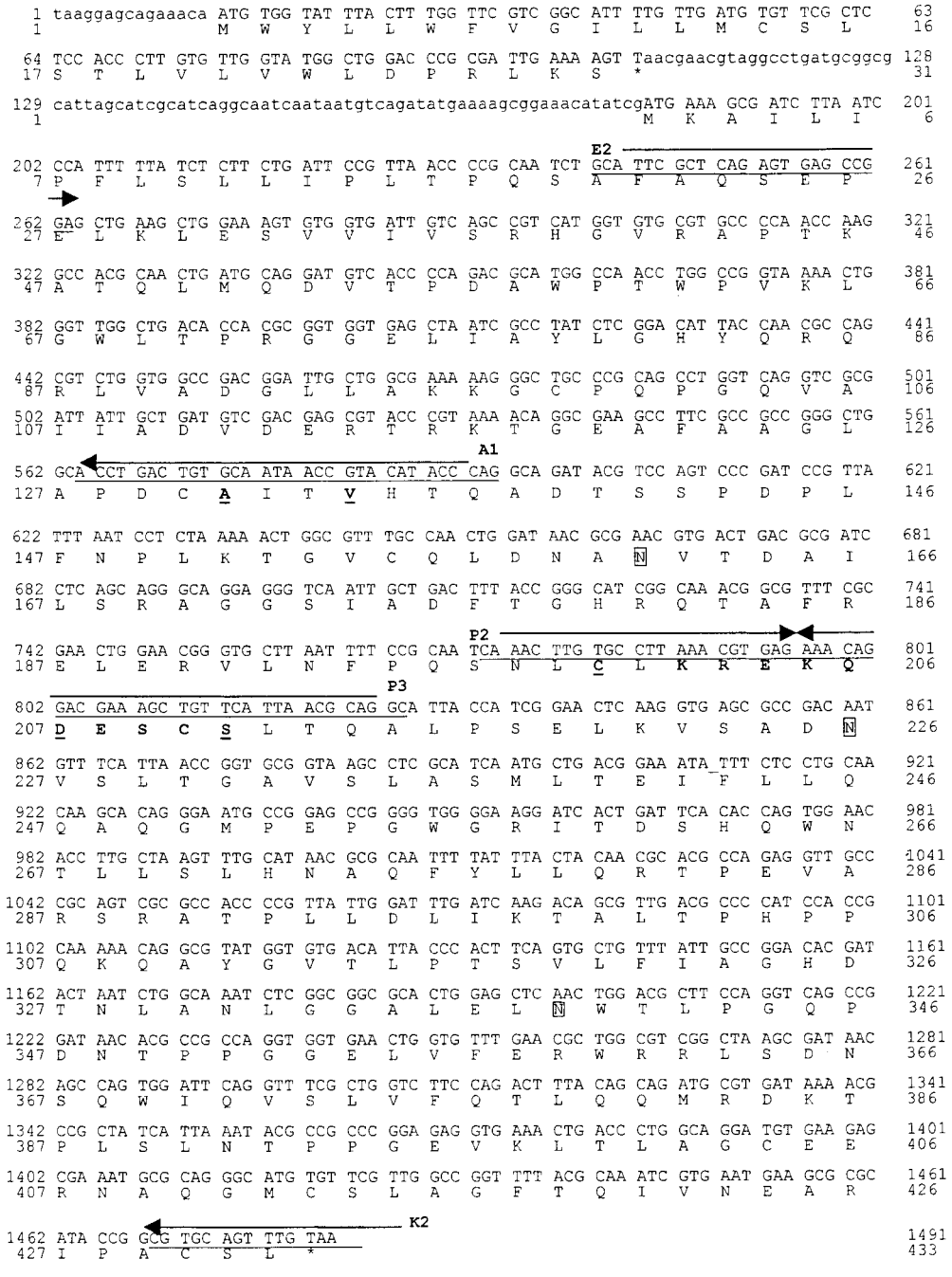

FIG. 1. Nucleotide and the deduced amino acid sequence of the *E. coli* acid phosphatase (appA). Primers are underlined and indicated by arrows. The GH loop region (202–211) is in bold and C200 (in G helix) and C210 (in GH loop) form the unique disulfide bond in the α-domain. Substituted amino acids (A131, V134N, C200, D207, and S211) are underlined and in bold.

the purified megaprimer (50 ng to 4 μg), depending on its size. Five thermal cycles were set up at 94°C for 1 min and 70°C for 2 min. While at 70°C, 1 μmol of forward primer and 2 U of AmpliTaq DNA polymerase were added and gently mixed with the reaction, and thermal cycling was continued for 25 times at 94°C for 1 min, 56°C for 1 min, and 70°C for 1.5 min.

Subcloning and expression. *E. coli* strain TOP10F′ (Invitrogen, San Diego, CA) was used as an initial host. The PCR fragments were purified and cloned into pGEMT-Easy vector (Promega) according to the manufacturer's instructions. *Eco*RI digestion of the isolated plasmid DNA was used to screen for positive transformants. The resulting inserts were cloned into pPICZαA (Kit Easy-select, Invitrogen) at the *Eco*RI site and transformed into TOP10F′ cells plated on LB medium containing 25 μg/mL zeocin. Colonies with desired inserts in the correct orientations were selected using *Sal*I or *Bst*XI restriction digestions of plasmid DNA. *Pichia pastoris* strain X33 (Mut$^+$ His$^+$) was used as the host for protein expression (Invitrogen) and grown in YPD liquid medium prior to electroporation. Two micrograms of

TABLE II

E. coli AppA Mutant Denomination and Construction

	Construct[a]	Size (bp)	Number of glycosylations
Mutants			
A131N/V134N/D207N/S211N	E2A1P3K2	1350	7
C200N/D207N/S211N	E2P2P3K2	1350	5
A131N/V134N/C200N/D207N/S211N	E2A1P2P3K2	1350	7
Wild type			
r-AppA	E2K2	1350	3

[a] See Table I for primer denomination.

plasmid DNA was linearized using restriction enzyme *Bgl*II or *Pme*I and then transformed into X33 according to the manufacturer's instructions (Invitrogen). After selected transformants were incubated in minimal media with glycerol (GMGY) for 24 h, 0.5% methanol medium (GMMY) was used to induce protein expression.

Enzyme purification and biochemical characterization. The expressed r-AppA and mutant enzymes in the medium supernatant were subjected to a two-step ammonium sulfate precipitation (25 and 75%) as previously described (25). The suspension of the first round was centrifuged at 4°C, 25,000*g* for 20 min. The pellet of the second round was suspended in 10 mL and dialyzed overnight against 25 mM Tris–HCl, pH 7. After dialysis, the protein extract was loaded onto a DEAE–Sepharose column (Sigma, St. Louis, MO) equilibrated with 25 mM Tris–HCl, pH 7. The bound protein was eluted with 1 M NaCl in 25 mM Tris–HCl, pH 7. Those three fractions exhibiting the highest activities were pooled and dialyzed against 25 mM Tris–HCl, pH 7.5, for the following analysis. Phytase activity was measured using sodium phytate as the substrate (25, 26). The enzyme was diluted in 0.25 M glycine–HCl, pH 2.5, and an equal volume of substrate solution containing 11 mM sodium phytate (Sigma) was added. After incubation of the sample for 15 min at 37°C, the reaction was stopped by addition of an equal volume of 15% trichloroacetic acid. Free inorganic phosphorus was measured at 820 nm after 0.2 mL of the sample was mixed with 1.8 mL of H_2O and 2 mL of a solution containing 0.6 M H_2SO_4, 2% ascorbic acid, and 0.5% ammonium molybdate, followed by incubation for 20 min at 50°C. One phytase unit was defined as the amount of activity that releases 1 μmol of inorganic phosphorus from sodium phytate per minute at 37°C. The final concentrations of sodium phytate used for the enzyme kinetics were 0.1, 0.25, 0.5, 0.75, 1, 2.5, 10, and 25 mM. Acid phosphatase activity was assayed using pNPP (Sigma) at a final concentration of 25 mM (24). To 50 μL of enzyme (40 nmol), 850 μL of 250 mM glycine–HCl, pH 2.5, was added. After 5 min of incubation at 37°C, 100 μL of pNPP was added. The released *p*-nitrophenol was measured at 405 nm after 0.1 mL of the sample was mixed with 0.9 mL of 1 M NaOH and incubated for 10 min. The final concentrations of pNPP used for the enzyme kinetics were 0.1, 0.2, 0.75, 1, 2.5, 10, and 25 mM. One unit of acid phosphatase activity was defined as the amount of enzyme catalyzing the formation of 1 μmol of *p*-nitrophenol per minute. Before the thermostability assay, the enzyme (2 mg/mL) was diluted 1:400 in 0.2 M glycine–HCl, pH 2.5. The diluted samples were incubated for 15 min at 25, 55, 80, and 90°C. After the samples were cooled on ice for 30 min, their remaining phytase activities were measured as described above. Deglycosylation of purified enzymes was done by incubating 100 μg of total protein with 0.5 IU endoglycosidase H_f (Endo H_f) for 4 h at 37°C according to the manufacturer's instructions (New England Biolabs, Beverly, MA). Sodium dodecyl sulfate–polyacrylamide gel electrophoresis (SDS–PAGE), 15% (w/v) gel, was performed as previously described (27). Protein concentrations were determined using the Lowry method (28).

Statistical analysis. Data were analyzed using SAS (release 6.04, SAS Institute, Cary, NC).

RESULTS

Effects of site-directed mutagenesis on phytase expression and glycosylation. Genomic DNA from each yeast transformant was extracted to amplify the desired mutated *appA* by PCR using E2 and K2 primers. All the desired mutations were confirmed by sequencing. For each mutant, 24 colonies were analyzed for phytase activity at various times after induction. All of the three mutants, A131N/V134N/D207N/S211N, C200N/D207N/S211N, and A131N/V134N/C200N/D207N/S211N, along with r-AppA, were expressed and secreted, resulting in a time-dependent accumulation of extracellular phytase activity that reached plateau at 96 h after methanol induction. The plateau activity in the medium supernatant was 35, 175, 57, and 117 U/mL, respectively (Table III). Yeast X33 transformed with the expression vector pPICZαA was used as a control and did not give any activity or phytase protein in SDS–PAGE (data not shown). On the purified protein basis, mutant C200N/D207N/S211N had the highest specific phytase activity, 63 U/mg, followed by mutant A131N/V134N/C200N/D207N/S211N, r-AppA, and mutant A131N/V134N/D207N/S211N (51, 41, and 32 U/mg of protein, respectively). The protein yield recovered after purification was 654, 324, 688, and 425 mg/L for the mutants C200N/D207N/S211N and A131N/V134N/C200N/D207N/S211N, r-AppA, and mutant A131N/V134N/D207N/S211N, respectively (Table III).

In SDS–PAGE, the band size of the purified r-AppA was 50–56 kDa, while that of mutant A131N/V134N/D207N/S211N was 68–70 kDa and that of mutant A131N/V134N/C200N/D207N/S211N was 86–90 kDa (Fig. 2). This gave an enhancement of the glycosylation level from 14% in r-AppA to 48% in mutant A131N/V134N/D207N/S211N and 89% in mutant A131N/V134N/C200N/D207N/S211N. The level of glycosylation in mutant C200N/D207N/S211N appeared equivalent to that of r-AppA. All of these recombinant

TABLE III

Phytase Yield and Specific Activity of r-AppA and the Three Mutants

	Phytase activity[a]	Protein yield[b]	Specific activity[c]	
			−Endo H_f	+Endo H_f
r-AppA	117 ± 15	688 ± 44	41 ± 3	37 ± 4
A131N/V134N/D207N/S211N	35 ± 4	425 ± 26	32 ± 2	29 ± 2
C200N/D207N/S211N	175 ± 19	654 ± 39	63 ± 4*	65 ± 5*
A131N/V134N/C200N/D207N/S211N	57 ± 8	324 ± 18	51 ± 5	46 ± 6

[a] Phytase activity (U/ml) in GMMY media after 96 h of culture.
[b] Protein yield (milligrams of purified protein per liter of culture).
[c] Specific phytase activity (units per milligram of purified protein).
* Indicates significant difference ($P < 0.05$) versus the r-AppA control. Results are representative of three experiments.

enzymes showed similar molecular mass, 45–48 kDa, after deglycosylation by Endo H_f. Deglycosylation did not significantly affect the specific activity of all the mutants or r-AppA (Table III). However, treating these purified proteins with both β-mercaptoethanol and Endo H_f caused a complete loss of phytase activity (data not shown).

Effects of site-directed mutagenesis on phytase pH and temperature optima and thermostability. Although all three mutants shared the same pH optimum (2.5) with that of r-AppA, mutant C200N/D207N/S211N was more ($P < 0.05$), while mutant A131N/V134N/C200N/D207N/S211N was less ($P < 0.05$), active than r-AppA at pH 3.5, 4.5, and 5.5 (Fig. 3). The temperature optimum was 65°C for mutant C200N/D207N/S211N and 55°C for the other two mutants and r-AppA (data not shown). In 0.2 M glycine–HCl, pH 2.5, mutant C200N/D207N/S211N exhibited a higher ($P < 0.05$) residual phytase activity than that of r-AppA after being heated at 80 and 90°C for 15 min (Fig. 4).

Effects of site-directed mutagenesis on enzyme kinetics. The K_m value for pNPP was reduced by one-half and the one for sodium phytate by 70% with mutant C200N/D207N/S211N, versus r-AppA ($P < 0.05$) (Table IV). Consequently, this mutant demonstrated a 1.9-fold increase in its apparent catalytic efficiency k_{cat}/K_m for pNPP and a 5.2-fold increase for sodium phytate relative to that of r-AppA. Although the k_{cat}/K_m values for mutant A131N/V134N/C200N/D207N/

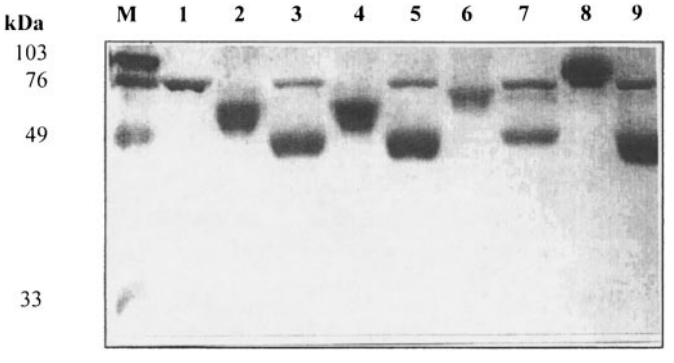

FIG. 2. SDS–gel electrophoresis (15%) of purified recombinant proteins expressed in *P. pastoris*. Thirty micrograms of protein was loaded per lane. Lane M, prestained marker (Bio-Rad, kDa) (phosphorylase *b*, 103; bovine serum albumin, 76; ovalbumin, 49; carbonic anhydrase, 33.2; soybean trypsin inhibitor, 28); lane 1, Endo H_f; lane 2, r-AppA; lane 3, r-AppA + Endo H_f; lane 4, mutant C200N/D207N/S211N; lane 5, mutant C200N/D207N/S211N + Endo H_f; lane 6, mutant A131N/V134N/D207N/S211N; lane 7, mutant A131N/V134N/D207N/S211N + Endo H_f; lane 8, mutant A131N/V134N/C200N/D207N/S211N; lane 9, mutant A131N/V134N/C200N/D207N/S211N + Endo H_f.

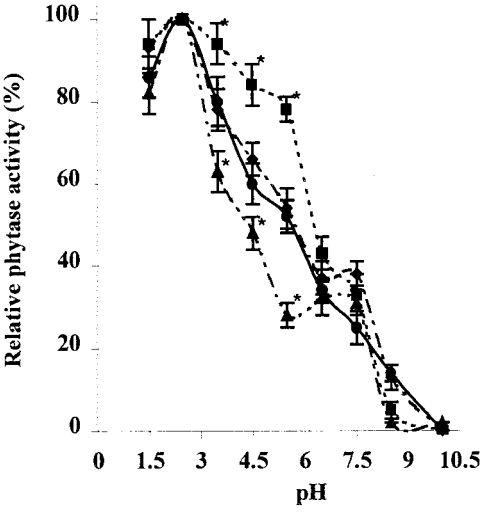

FIG. 3. pH dependence of the enzymatic activity at 37°C of the purified r-AppA (●) and mutants (C200N/D207N/S211N, ■; A131N/V134N/C200N/D207N/S211N, ▲; A131N/V134N/D207N/S211N, ◆) using sodium phytate as a substrate. The maximal activity for each mutant and r-AppA was defined as 100%. Buffers: pH 1.5–3.5, 0.2 M glycine–HCl; pH 4.5–7.5, 0.2 M sodium citrate; pH 8.5–11, 0.2 M Tris–HCl. Asterisks indicate significant differences ($P < 0.05$) between r-AppA and other mutants. Results are expressed as the mean ± SE from three experiments.

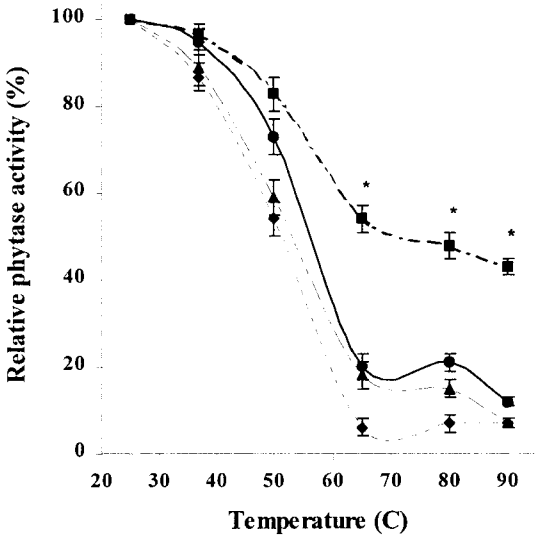

FIG. 4. Residual enzymatic activity of the purified r-AppA (●) and mutants (C200N/D207N/S211N, ■; A131N/V134N/C200N/D207N/S211N, ▲; A131N/V134N/D207N/S211N, ◆) after exposure for 15 min at the indicated temperature. The purified enzyme was incubated for 15 min in 0.2 M glycine–HCl, pH 2.5. At the end of heating, the reaction mixture was cooled on ice for 30 min. The initial activity with sodium phytate for each recombinant enzyme was defined as 100%. Asterisks indicate significant differences ($P < 0.05$) between r-AppA and other mutants. Results are expressed as the mean ± SE from three experiments.

S211N were also significantly different from those of r-AppA for sodium phytate, the actual enhancement was relatively small. In contrast, mutant A131N/V134N/D207N/S211N demonstrated a significantly lower catalytic efficiency than that of r-AppA for both substrates.

DISCUSSION

Our results indicate that additional N-glycosylation sites can be added to EcAP by site-directed mutagenesis. Compared with the r-AppA produced by the intact *appA* gene, the mutant enzymes A131N/V134N/D207N/S211N and A131N/V134N/C200N/D207N/S211N clearly demonstrated enhanced glycosylation, as shown by their differences in molecular masses before and after deglycosylation. Thus, the engineered N-glycosylation sites in these two mutants were indeed recognized by *P. pastoris* and processed correctly. Because of the multiple mutations in mutants A131N/V134N/D207N/S211N and A131N/V134N/C200N/D207N/S211N, our results cannot assess the level of glycosylation at specific engineered sites, but useful information can be derived by comparisons between the mutants and r-AppA. First, although both mutants A131N/V134N/D207N/S211N and A131N/V134N/C200N/D207N/S211N had four additional N-glycosylation sites with respect to r-AppA, mutant A131N/V134N/C200N/D207N/S211N displayed more than 40% of N-glycosylation than A131N/V134N/D207N/S211N (89 vs 48%). Because the substitution C200N in mutant A131N/V134N/C200N/D207N/S211N was the only difference between these two variants and that mutation added no additional putative N-glycosylation site, it seems that changing C200N itself might enhance *N*-glycosylation at certain sites. Second, although mutant C200N/D207N/S211N had two additional *N*-glycosylation sites (N207 and N211), its apparent molecular weight was the same as that of r-AppA, suggesting the two engineered glycosylation sites in mutant C200N/D207N/S211N were silent. This demonstrates that although the presence of such a signal sequence is required for glycosylation, it does not necessarily result in glycosylation (29). Possibly, the residues mutated in the case of mutant C200N/D207N/S211N were not as solvent accessible as our structure-based sequence alignment led us to believe. The recently published crystal structure of EcAP may help answer this question (22, 30). Lastly, mutant A131N/V134N/D207N/S211N had a significant increase in glycosylation compared with that of mutant C200N/D207N/S211N. The difference might be caused

TABLE IV

Catalytic Properties of r-AppA and the Three Mutants[a]

	p-Nitrophenyl phosphate			Sodium phytate		
	K_m (mM)	k_{cat} (min^{-1})	k_{cat}/K_m (min^{-1} M^{-1})	K_m (mM)	k_{cat} (min^{-1})	k_{cat}/K_m (min^{-1} M^{-1})
r-AppA	3.66 ± 0.44	752 ± 7.9	$(2.0 \pm 0.18) \times 10^5$	1.95 ± 0.25	2148 ± 33	$(1.11 \pm 0.13) \times 10^6$
A131N/V134N/D207N/S211N	7.87 ± 0.84*	390 ± 5.9*	$(0.5 \pm 0.07) \times 10^5$*	3.07 ± 0.26*	1657 ± 23*	$(0.54 \pm 0.09) \times 10^6$*
C200N/D207N/S211N	1.86 ± 0.35*	1073 ± 13*	$(5.8 \pm 0.37) \times 10^5$*	0.58 ± 0.08*	4003 ± 56*	$(6.90 \pm 0.70) \times 10^6$*
A131N/V134N/C200N/D207N/S211N	3.18 ± 0.39	787 ± 6.7	$(2.5 \pm 0.17) \times 10^5$	2.03 ± 0.19	3431 ± 41*	$(1.69 \pm 0.21) \times 10^6$*

[a] Reaction velocity measurements were performed in triplicate as described in the text. The values for K_m were calculated using the Lineweaver–Burk plot method. All reactions were measured in 0.25 M glycine–HCl, pH 2.5.

* Indicates significant difference ($P < 0.05$) versus the r-AppA control. Results are representative of five independent experiments.

by the two added *N*-glycosylation sites at A131N and V134N in mutant A131N/V134N/D207N/S211N. Given the above results, we can make the following observations: (1) the substitutions A131N and V134N result in increased glycosylation of EcAP; (2) the substitutions D207N and S211N were silent; (3) the substitution C200N appeared to enhance glycosylation at other sites in the case of mutant A131N/V134N/C200N/D207N/S211N, but not in mutant C200N/D207N/S211N.

In general, additional glycosylation of proteins has been shown to facilitate folding and increase stability (31, 32). Our main goal in this study was to improve the thermostability of r-AppA by enhancing its glycosylation level. Contrary to our expectations, mutants A131N/V134N/D207N/S211N and A131N/V134N/C200N/D207N/S211N did not demonstrate enhanced thermostability, despite elevated levels of glycosylation. Surprisingly, mutant C200N/D207N/S211N displayed a greater thermostability despite having the same level of glycosylation as r-AppA. Although performing C200N does not mean that N-glycosylation at other sites has occurred, greater glycosylation at specific sites is feasible. Seemingly, the mutations per se rather than the total level of glycosylation had contributed to this effect. A recent study described the production of six different phytases expressed in either *Aspergillus niger* or the yeast *Hansenula polymorpha* (33). The results indicated that levels of glycosylation depended on the host chosen, but had no significant effect on thermostability, specific activity, or protein refolding (33).

The kinetic data indicate that all three mutants and r-AppA had lower K_m and higher k_{cat}/K_m values for sodium phytate than for pNPP. Clearly, these recombinant enzymes have higher apparent efficiency for the former than the latter, supporting that EcAP is more a phytase than an acid phosphatase (22, 25). Mutant C200N/D207N/S211N exhibited the largest enhancement in its apparent efficiency for both substrates over that of r-AppA. The enhancement in k_{cat}/K_m is most likely due to a large decrease in K_m (1.86 vs 3.66 mM for pNPP and 0.58 vs 1.95 mM for sodium phytate). This means that the mutant C200N/D207N/S211N is saturated at a lower concentration of substrate than r-AppA. In addition, there was also a significant difference in k_{cat} for both substrates between these two forms of phytase. Based on the structure of rat acid phosphatase (18), these mutations do not seem to be involved in the enzyme active site or the formation of acid phosphatase dimer (data not shown). Probably, these mutations singly or jointly affect the conformational flexibility of the enzyme, such as described previously for another protein (34). Based on the recently solved crystal structures of *E. coli* phytase (22, 30), none of our mutations are directly involved in the substrate-binding pocket. However, C200 and C210, labeled as C178 and C188 by Lim *et al.* (22), are involved in a disulfide bond between helix G and the GH loop in the α-domain of the protein (22). With the mutation C200N, the unique disulfide bond into the α-domain is no longer present in the GH loop. This change may result in a better flexibility of the α-domain toward the central cavity or "substrate-binding site" of the enzyme (22). This internal flexibility may be also supported by the fact that mutant C200N/D207N/S211N, and to a lesser extent mutant A131N/V134N/C200N/D207N/S211N, demonstrated an improvement in the catalytic efficiency for sodium phytate hydrolysis. Since there was no enhanced glycosylation for mutant C200N/D207N/S211N, our engineered glycosylation sites N207 and N211, labeled as D185 and S189 by Lim *et al.* (22), may be masked from the exposed surface. The improvement of thermostability for mutant C200N/D207N/S211N may be therefore explained by an increasing number of hydrophobic interactions not presented in mutant A131N/V134N/C200N/D207N/S211N or A131N/V134N/D207N/S211N.

It is worth mentioning that the specific activities of phytase in all three mutants and r-AppA were not significantly affected by deglycosylation. However, deglycosylation, as shown in glycoprotein hormones (14) or the *Schwanniomyces occidentalis* α-amylase expressed in *S. cerevisiae* (15), may be associated with possible conformational changes that modulate the substrate binding and (or) the velocity of its utilization. All of the mutants and the intact control were completely inactivated by both β-mercaptoethanol and deglycosylation treatments. This suggests that the four disulfide bonds play altogether a key role in maintaining the catalytic function of these recombinant phytases (35).

In conclusion, when the G helix and the GH loop do not contain the disulfide bond C200/C210 in the mutant C200N/D207N/S211N, the α-domain may become slightly more flexible, resulting a positive modulation on the catalytic efficiency and the thermostability of the enzyme. Because the *E. coli* phytase crystal structure will be released in the near future (22), more targeted mutagenesis studies should shed light on conformational changes that may improve the properties of the enzyme.

ACKNOWLEDGMENTS

We thank Obdulio Piloto for his assistance in laboratory analysis. This research was supported by a project of the Cornell Biotechnology Program, New York State Science and Technology.

REFERENCES

1. Reddy, N. R., Sathe, S. K., and Salunkhe, D. K. (1982) *Adv. Food Res.* **28,** 1–92.
2. Dassa, E., Cahu, M., Desjoyaux-Cherel, B., and Boquet, P. L. (1982) *J. Biol. Chem.* **257,** 6669–6676.

3. Dassa, J., Marck, C., and Boquet, P. L. (1990) *J. Bacteriol.* **172,** 5497–5500.
4. Ostanin, K., and Van Etten, R. L. (1993) *J. Biol. Chem.* **268,** 20778–20784.
5. Ostanin, K., Harms, E. H., Stevis, P. E., Kuciel, R., Zhou, M. M., and Van Etten, R. L. (1992) *J. Biol. Chem.* **267,** 22830–22836.
6. Rodriguez, E., Porres, J. M., Han, Y. M., and Lei, X. G. (1999) *Arch. Biochem. Biophys.* **365,** 262–267.
7. Stahl, C. H., Han, Y. M., Roneker, K. R., House, W. A., and Lei, X. G. (1999) *J. Anim. Sci.* **77,** 2135–2142.
8. Jongbloed, A. W., Lenis, N. P., and Mroz, Z. (1997) *Vet. Q.* **19,** 130–134.
9. Han, Y. M., Wilson, D. B., and Lei, X. G. (1999) *Appl. Environ. Microbiol.* **65,** 1915–1918.
10. Han, Y. M., and Lei, X. G. (1999) *Arch. Biochem. Biophys.* **364,** 83–90.
11. Keutmann, H. T., Johnson, L., and Ryan, R. J. (1985) *FEBS Lett.* **185,** 333–338.
12. Kornfeld, R., and Kornfeld, S. (1985) *Annu. Rev. Biochem.* **54,** 631–664.
13. Kwon, K. S., Song, M., and Yu, M. H. (1995) *J. Biotechnol.* **42,** 191–195.
14. Terashima, M., Kubo, A., Suzawa, M., Itoh, Y., and Katoh, S. (1994) *Eur. J. Biochem.* **226,** 249–254.
15. Yanez, E., Carmona, T. A., Tiemblo, M., Jimenez, A., and Fernandez-Lobato, M. (1998) *Biochem. J.* **329,** 65–71.
16. Kern, G., Schulke, N., Schmidt, F. X., and Jaenicke, R. (1992) *Protein Sci.* **1,** 120–131.
17. Matthews, B. W. (1993) *Annu. Rev. Biochem.* **62,** 139–160.
18. Schneider, G., Lindqvist, Y., and Vihko, P. (1993) *EMBO J.* **12,** 2699–2715.
19. Smith, A. M., and Klugman, K. P. (1997) *Biotechniques* **22,** 438–442.
20. Luthy, R., McLachlan, A. D., and Eisenberg, D. (1996) *Proteins* **10,** 229–239.
21. Kabsch, W., and Sander, C. (1983) *Biopolymers* **22,** 2577–2637.
22. Lim, D., Golovan, S., Forsberg, C. W., and Jia, Z. (2000) *Nat. Struct. Biol.* **7,** 108–113.
23. Seraphin, B., and Kandels-Lewis, S. (1996) *Nucleic Acids Res.* **24,** 3276–3277.
24. Smith, R. F., and Smith, T. F. (1992) *Protein Eng.* **5,** 35–41.
25. Rodriguez, E., Han, Y. M., and Lei, X. G. (1999) *Biochem. Biophys. Res. Commun.* **257,** 117–123.
26. Piddington, C. S., Houston, C. S., Paloheimo, M., Cantrell, M., Miettinen-Oinonen, A., Nevalainen, H., and Rambosek, J. (1993) *Gene* **133,** 55–62.
27. Laemmli, U. K. (1970) *Nature* **227,** 680–685.
28. Lowry, O. H., Rosebrough, N. J., Farr, A. L., and Randall, R. J. (1951) *J. Biol. Chem.* **193,** 265–275.
29. Meldgaard, M., and Svendsen, I. (1994) *Microbiology* **140,** 159–166.
30. Jia, Z., Golovan, S., Ye, Q., and Forsberg, C. W. (1998) *Acta Crystallogr., D: Biol. Crystallogr.* **54,** 647–649.
31. Haraguchi, M., Yamashiro, S., Furukawa, K., Takamiya, K., Shiku, H., and Furukawa, K. (1995) *Biochem. J.* **312,** 273–280.
32. Imperiali, B., and Rickert, K. W. (1995) *Proc. Natl. Acad. Sci. USA* **92,** 97–101.
33. Wyss, M., Pasamontes, L., Friedlein, A., Remy, R., Tessier, M., Kronenberger, A., Middendorf, A., Lehmann, M., Schnoebelen, L., Rothlisberger, U., Kusznir, E., Wahl, G., Miller, F., Lahm, H. W., Vogel, K., and van Loon, A. P. G. M. (1999) *Appl. Environ. Microbiol.* **65,** 359–366.
34. Kern, G., Kern, D., Jaenicke, R., and Seckler, R. (1993) *Protein Sci.* **2,** 1862–1868.
35. Ullah, A. H., and Mullaney, E. J. (1996) *Biochem. Biophys. Res. Commun.* **227,** 311–317.